

Article

Conformational and Chiroptical Properties of Salicylamide-Based Peptidomimetics

Ivan Raich ^{1,*} , Karel Pauk ², Ales Imramovsky ²  and Josef Jampilek ^{3,4} 

¹ Department of Chemistry of Natural Compounds, Faculty of Food and Biochemical Technology, University of Chemistry and Technology in Prague, Technicka 5, 166 28 Prague 6, Czech Republic

² Institute of Organic Chemistry and Technology, Faculty of Chemical Technology, University of Pardubice, Studentska 95, 530 09 Pardubice, Czech Republic; karel.pauk@upce.cz (K.P.); ales.imramovsky@upce.cz (A.I.)

³ Department of Chemical Biology, Faculty of Science, Palacky University, Slechtitelu 27, 783 71 Olomouc, Czech Republic; josef.jampilek@gmail.com

⁴ Department of Analytical Chemistry, Faculty of Natural Sciences, Comenius University, Ilkovicova 6, 842 15 Bratislava, Slovakia

* Correspondence: ivan.raich@vscht.cz

Abstract: Optical rotation (OR), the most frequently used chiroptical method, is used for the characterization of newly synthesized or isolated compounds. Computational predictions of OR are, however, mainly used for the determination of the absolute configurations of chiral compounds, but they may also be used for the verification of conformational analysis results if the experimental values are known. Our computational study deals with the conformational analysis of flexible salicylamide-based peptidomimetics, starting with a conformation search, then a low-level *ab initio* preoptimization of the hundreds of conformations found, and, finally, a higher-level DFT optimization. For the resulting minima structures, Boltzmann populations were calculated, followed by OR calculations for all the populated conformers using the DFT method with various basis sets with diffuse functions. Weighted averages of the ORs were compared with experimental values, and the agreement, which ranged from excellent to moderate for various compounds, served as a verification of the conformational analysis results.

Keywords: salicylamide; peptidomimetics; antimicrobial activity; optical rotation; absolute configuration; conformational analysis; DFT calculations



Citation: Raich, I.; Pauk, K.; Imramovsky, A.; Jampilek, J.

Conformational and Chiroptical Properties of Salicylamide-Based Peptidomimetics. *Symmetry* **2024**, *16*, 138. <https://doi.org/10.3390/sym16020138>

Academic Editor: Angela Patti

Received: 11 December 2023

Revised: 18 January 2024

Accepted: 22 January 2024

Published: 24 January 2024



Copyright: © 2024 by the authors. Licensee MDPI, Basel, Switzerland. This article is an open access article distributed under the terms and conditions of the Creative Commons Attribution (CC BY) license (<https://creativecommons.org/licenses/by/4.0/>).

1. Introduction

Knowing the exact spatial arrangement of compounds, either newly synthesized or isolated from natural sources, is fundamental knowledge for the study of their properties not only in the pharmaceutical industry and medicine but also in organic chemistry, biochemistry, and materials science [1–8]. Furthermore, for chiral compounds, the absolute configuration must be known. Common structure determination techniques like NMR, IR, or MS spectroscopy cannot be used for this purpose, as two enantiomers provide the same spectral signals in all these spectroscopies. The only classical structural tool that can distinguish enantiomers is X-ray crystallography, which is, however, limited to crystalline compounds only. Here, the recently developed computational methods may be of use, as *ab initio* or DFT calculations of chiroptical properties may be used for the determination or confirmation of the absolute configurations of chiral compounds. And as optical rotation (OR) is a routinely measured property for new compounds, the calculation of OR is the most frequently used method for that purpose, making use of the fact that the ORs of both enantiomers E_R and E_S are of the same absolute value but of opposite signs:

$$[\alpha]_v(E_R) = -[\alpha]_v(E_S) \quad (1)$$

The theoretical quantum-mechanical background for optical rotation was derived long ago by Rosenfeld in 1928 [9], and the current methodology has been reviewed recently [10,11]. As a result, calculations of OR for rigid molecules are becoming routine. However, for conformationally flexible molecules, the situation is more complicated, and a detailed conformational analysis must be performed prior to OR calculations to obtain equilibrium populations of stable conformations and their relative free energies. The calculated OR is then a weighted average of the ORs of populated conformers:

$$[\alpha]_v = \sum_i x_i [\alpha]_v^i \quad (2)$$

where x_i is the molar fraction of the i -th conformer and $[\alpha]_v^i$ is the optical rotation of the i -th conformer.

OR is extremely sensitive to the shape of a molecule, and even different conformers of the same compound often have different signs of OR. Comparison of experimental and calculated value of OR can thus be used as a verification of the results of conformational analysis.

For our computational study, six compounds bearing the salicylic motif, which are interesting both for their structure and spectrum of biological activities, were selected. Salicylic acid is found, for example, in willow bark, from which it was isolated. In addition to fulfilling the function of a plant hormone [12], today, it is mainly used in dermatology [13]; however, its antimicrobial activity has also been described [14–16]. The best-known drugs derived from it are acetylsalicylic acid or Aspirin[®]—with anti-inflammatory, antipyretic, and anticoagulant effects [17]—and mesalazine, which is used to treat inflammatory bowel diseases [18]. Salicylanilides, commercially available, e.g., as niclosamide [19], rafxanide [20], or closantel [21], are anthelmintics, but in recent years, their other biological effects have been discovered, e.g., anticancer [22] or antiviral [23], stimulating scientific interest in these simple and small molecules [24–32]. In addition to anticancer activity [33], for example, their herbicidal activity [34] or ability to inhibit acetylcholinesterase [35–37] can be mentioned. However, the antimicrobial activity of salicylamides is the most described [24,25,38–46], and it can be multiplied by introducing a carbamate group to the free phenolic salicylic hydroxyl or by inserting an amino acid fragment between the salicylic and anilide parts of the molecule, i.e., by the preparation of diamides, namely, salicylamide-based peptidomimetics [30,47–53]. It is necessary to mention that salicylanilide-based peptidomimetics also show anticancer activity [54–56].

2. Materials and Methods

2.1. Compounds

Structures of all six salicylamides 1–6 under study are given in Table 1 together with their systematic names generated using ACD/Name ver. 12.01 software [57]. Their synthesis, spectral data, optical rotations, and biological activities were described previously [30,47,52] (and refs. thereon).

Table 1. Structures of salicylamides.

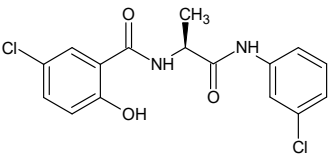
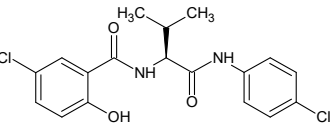
Comp.	Structure	Name	Molecular Formula /Weight	Refs.
1		5-chloro- <i>N</i> -{[(2 <i>S</i>)-1-[(3-chlorophenyl)amino]-1-oxopropan-2-yl]-2-hydroxybenzamide	C ₁₆ H ₁₄ Cl ₂ N ₂ O ₃ [353.200]	[30,47]
2		5-chloro- <i>N</i> -{[(2 <i>S</i>)-1-[(4-chlorophenyl)amino]-3-methyl-1-oxobutan-2-yl]-2-hydroxybenzamide	C ₁₈ H ₁₈ Cl ₂ N ₂ O ₃ [381.253]	[47]

Table 1. Cont.

Comp.	Structure	Name	Molecular Formula /Weight	Refs.
3		5-chloro-2-hydroxy-N-((2S)-3-methyl-1-[(4-methylphenyl)amino]-1-oxobutan-2-yl)benzamide	C ₁₉ H ₂₁ ClN ₂ O ₃ [360.835]	[30,47]
4		5-chloro-2-hydroxy-N-((2S)-1-[(4-methoxyphenyl)amino]-3-methyl-1-oxobutan-2-yl)benzamide	C ₁₉ H ₂₁ ClN ₂ O ₄ [376.834]	[30,47]
5		5-chloro-2-hydroxy-N-((2S)-3-methyl-1-[(4-nitrophenyl)amino]-1-oxobutan-2-yl)benzamide	C ₁₈ H ₁₈ ClN ₃ O ₅ [391.806]	[30]
6		5-chloro-2-hydroxy-N-[(2S)-3-methyl-1-oxo-1-[[4-(trifluoromethyl)phenyl]amino]butan-2-yl]benzamide	C ₁₉ H ₁₈ ClF ₃ N ₂ O ₃ [414.806]	[30,47]

2.2. Conformational Analysis and Geometry Optimizations

Low-energy conformers for all compounds **1–6** were searched using the Conformational Search routine of HyperChem ver. 8.0.3 software [58] at the molecular mechanics level using the MM+ forcefield. Found structures were preoptimized at the HF/4-31G level in a gas phase. Final optimization of all resulting geometries was performed at the DFT level using the hybrid B3PW91 [59,60] functional with 6-31G(d,p) basis set in chloroform using the CPCM [61,62] implicit solvation model. For comparison, final optimizations were also performed with the same DFT functional augmented with the D3 version of Grimme's dispersion correction [63]. All minima were confirmed by a frequency calculation at the same level of theory, and Boltzmann populations of each conformer p_i were calculated using

$$p_i = \frac{\exp\left(-\frac{\epsilon_i}{kT}\right)}{\sum_i \exp\left(-\frac{\epsilon_i}{kT}\right)} \quad (3)$$

where ϵ_i is the Gibbs free energy of i -th conformer, k is the Boltzmann constant, and T is the absolute temperature. All DFT calculations were performed using the Gaussian 16 package [64].

2.3. Calculations of Optical Rotation

Experimental optical rotations were measured in ethyl acetate at the wavelength of sodium D line at 589 nm. Theoretical ORs were calculated in the same solvent and at the same wavelength using the B3PW91 functional and various basis sets with a polarization function.

3. Results and Discussion

3.1. Conformational Analysis

All salicylamides **1–6** are very flexible molecules with many freely rotatable bonds. Relevant low-energy conformations were searched using the conformation search utility in HyperChem software. The number of conformers found for each compound is given in Table 2. At a minimum, several hundred conformations were found for each compound, with a maximum of 1268 for compound **3**. For this reason, a low-level preoptimization was performed at the Hartree-Fock HF/4-31 level. This step reduced the number of conformations to about 20, and it is also given in Table 2.

Table 2. Results of conformation search and preoptimization.

Comp.	Conformations after Conformation Search	Conformations after Preoptimization
1	268	22
2	349	25
3	1268	10
4	1219	22
5	1180	13
6	518	24

Final geometry optimizations were performed at the B3PW91/6-31G(d,p) level. Originally, conformational analysis was intended for predictions of NMR and IR spectra, and chloroform was used as an implicit solvent using CPCM model. However, it was verified that there were only minor differences in the optimized geometries in ethyl acetate and in chloroform.

All local minima were verified through frequency calculations at the same theoretical level, and Boltzmann populations were calculated based on Gibbs free energies. Up to four populated conformers were found for compounds 1–6, and their geometries and populations are given in Table 3.

Table 3. Populated conformers after conformational analysis.

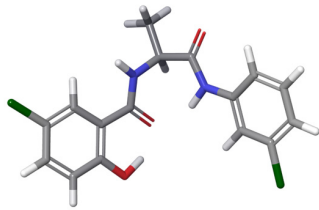
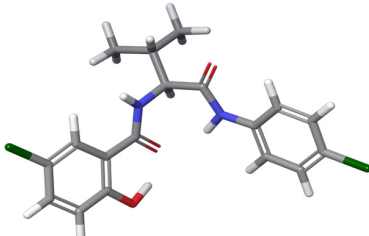
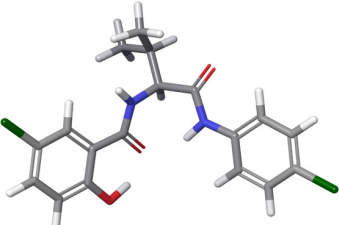
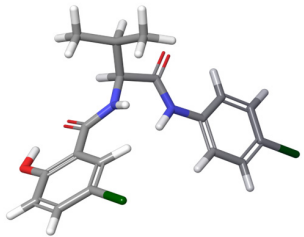
Comp.	Conformer Designation	Geometry	Population
1	a		99.95%
2	a		60.74%
	b		23.13%
	c		16.09%

Table 3. Cont.

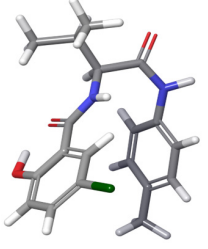
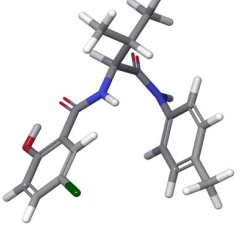
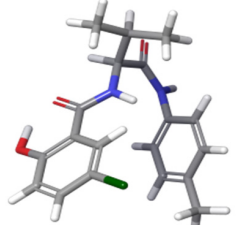
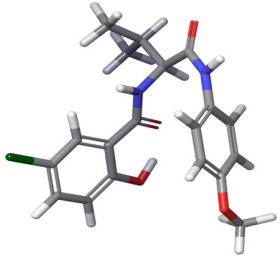
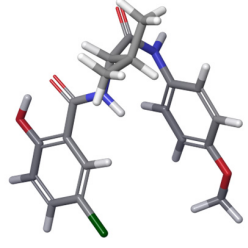
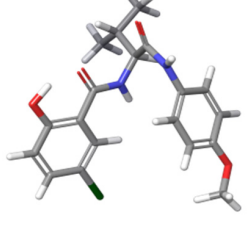
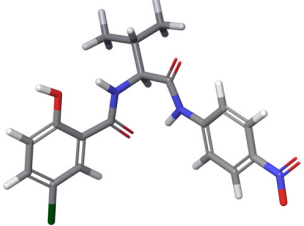
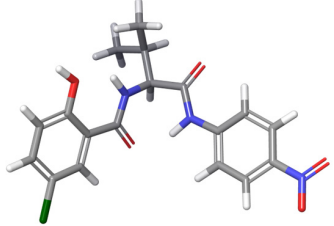
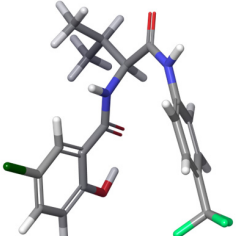
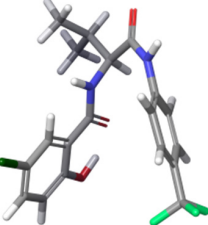
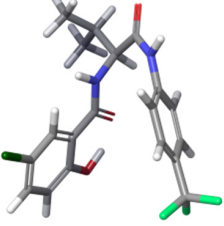
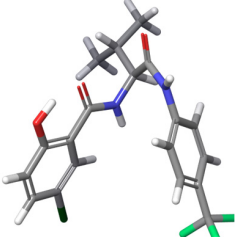
Comp.	Conformer Designation	Geometry	Population
3	a		79.29%
	b		16.40%
	c		4.30%
4	a		69.25% ^a
	b		17.52% ^a
	c		7.54% ^a

Table 3. Cont.

Comp.	Conformer Designation	Geometry	Population
5	a		67.90%
	b		32.09%
6	a		34.50%
	b		33.11%
	c		27.79%
	d		14.10%

^a For the calculation of weighted averages of ORs, populations were normalized to 100%.

The various conformers of each compound differ mainly in the torsion angles connecting both aromatic rings. They are designated according to Figure 1 and, for a better quantitative characterization of the separate conformers, are listed in Table 4.

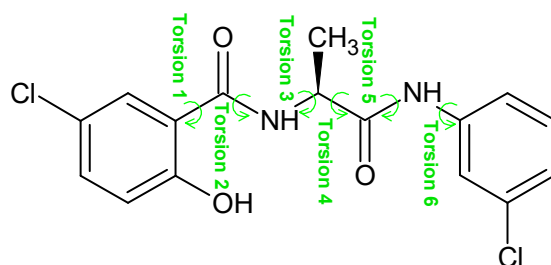


Figure 1. Designation of torsion angles.

Table 4. Torsion angles of populated conformers.

Conformer	Torsion 1	Torsion 2	Torsion 3	Torsion 4	Torsion 5	Torsion 6
1a	−169.7	−174.1	−87.4	67.0	−178.1	177.7
2a	−170.0	−177.6	−87.9	76.7	−176.4	174.6
2b	−168.7	−173.7	−88.1	61.4	−179.1	179.9
2c	172.9	−173.2	−117.5	12.8	176.7	−178.1
3a	173.1	−178.7	−132.6	41.4	16.1	51.4
3b	−173.7	−178.8	149.7	−37.1	−11.6	117.1
3c	−171.1	−174.1	−106.8	−3.6	−14.9	114.7
4a	−168.2	−178.6	−130.6	40.0	14.3	55.4
4b	−172.4	−178.1	−84.4	−43.2	−8.0	106.6
4c	−171.8	179.6	57.7	56.0	8.4	64.8
5a	1.3	−174.8	−86.8	72.1	−176.7	174.4
5b	0.4	−172.5	−85.9	60.0	−178.8	179.4
6a	−174.6	−176.2	−133.2	39.5	18.4	42.6
6b	174.0	−176.4	−133.8	39.4	16.9	43.7
6c	173.5	−176.9	−133.4	39.4	17.1	44.8
6d	171.2	176.2	55.2	51.5	6.8	52.4

To assess the effect of dispersion interactions, all final optimizations at the DFT level were also performed with the dispersion-corrected DFT method (DFT-D) [63] as included in Gaussian 16. This only led to minor changes in geometries and populations for compounds 1 and 2. However, for other compounds, the changes are more noticeable. Their populations and torsion angles are given in Table 5.

Table 5. Populations and torsion angles of dispersion-corrected populated conformers.

Conformer	Population	Torsion 1	Torsion 2	Torsion 3	Torsion 4	Torsion 5	Torsion 6
1a	92.17%	−164.8	−175.9	−85.5	65.3	−174.6	170.2
2a	48.37%	−166.2	−178.0	−87.0	73.9	−172.8	167.4
2b	29.67%	−164.4	−174.1	−87.0	58.7	−176.2	174.6
2c	11.36%	−164.2	167.4	−124.0	34.3	15.2	53.9
2d	8.45%	170.0	−174.1	−125.7	17.0	177.8	−179.1
3a	90.63%	−163.1	169.0	−125.9	36.2	14.3	−124.3
3b	7.32%	−164.8	172.2	−75.6	−7.3	−5.6	112.2
4a	95.70%	−164.8	169.0	−125.0	34.7	12.3	−132.2
4b	4.20%	−162.3	170.3	−59.6	−33.2	2.1	109.2
5a	94.07%	−167.5	164.4	−124.9	31.9	13.9	−131.6
5b	2.44%	162.5	−164.9	36.4	42.7	−10.8	−122.6
6a	89.84%	−167.0	166.3	−124.3	32.6	14.8	−129.2
6d	7.47%	−160.3	169.4	−56.3	−30.8	1.1	115.5

3.2. Calculations of Optical Rotation

For the calculation of optical rotation, we used the time-dependent Density Functional Theory (TDDFT) [65–68] methodology with gauge-invariant atomic orbitals (GIAOs) as implemented in Gaussian 16 software. Using a standard B3PW91 functional, we sought to test several basis sets with diffuse functions (6-311++G(2d,p), aug-cc-pVDZ, aug-cc-pVTZ, and aug-cc-pVQZ). To allow us to compare our calculated optical rotations with the experimental ones, the calculations were performed at the sodium D line wavelength, i.e., 589 nm.

While the substitution of an implicit solvent in the CPCM solvent model plays only a minor role during geometry optimization calculations, we noticed that it plays a significant role during OR calculation. Optical rotations are thus sensitive to solvents [69], even of similar polarity. Differences between the calculated optical rotations in chloroform and ethyl acetate for compounds **1** and **2** and several basis sets are illustrated in Table 6. The same geometry is used in both calculations. For comparison, experimental optical rotations are listed in Table 7.

Table 6. Calculated optical rotations using different solvents and basis sets.

Comp.	Solvent	6-311++G(2d,p)	aug-cc-pVDZ	aug-cc-pVTZ
1	chloroform	−0.4	6.9	14.0
	ethyl acetate	1.7	22.6	31.5
2	chloroform	−90.3	−85.1	−78.8
	ethyl acetate	−81.1	−73.9	−70.2

Table 7. Experimental optical rotations in ethyl acetate.

Comp.	$[\alpha]_D$	Refs.
1	37.0 (c 1.6)	[30,47]
2	−71.7 (c 1.5)	[47]
3	−56.2 (c 0.3)	[30,47]
4	−63.2 (c 0.2)	[30,47]
5	−64.8 (c 0.2)	[30]
6	−73.8 (c 0.2)	[30,47]

It is obvious that the optical rotations calculated in ethyl acetate were in all cases in better agreement with the experimental values compared to those in chloroform.

The optical rotations of all the populated conformers and their Boltzmann weighted averages calculated in ethyl acetate with various basis sets are given in Table 8.

The level of agreement of the calculated data with the experimental optical rotations differs for the various compounds. Structure **1**, which is conformationally rigid and for which only one populated conformer was found, provides, with triple- ζ and quadruple- ζ basis sets, an excellent agreement with the experimental value of 37.0°. For compound **2**, the best agreement was achieved even if it had three conformers, two of them having a negative value of ORs and one having a positive value. It is obvious that conformational analysis in this case provided an exact representation of the populated conformers. All the basis sets performed well for this structure, with, again, quadruple- ζ being the best. Compounds **3** and **4** showed similarly good agreement with the experimental values, with a difference of about 20°. Both compounds consist of three conformers of different signs of ORs, and the conformational analysis seems to provide an exact representation of the conformers. However, a trend of improving results with a larger basis set was not observed here. The worst agreement was observed for compounds **5** and **6**, with a difference of about 200 and 70°, respectively. Both compounds consist of conformers with large negative values of OR ($< -150^\circ$), and there is no way to achieve experimental values of about -70° . It is obvious that conformational analysis probably omitted some conformers with a more positive value of ORs for both compounds.

Table 8. Calculated optical rotations in ethyl acetate.

Comp.	Conformer	6-311++G(2d,p)	aug-cc-pVDZ	aug-cc-pVTZ	aug-cc-pVQZ
1	a	1.7	22.6	31.5	32.2
2	a	−98.6	−90.3	−84.5	−86.1
	b	−214.9	−207.0	−200.6	−203.2
	c	177.2	179.1	179.9	180.8
	w. a. ¹	−81.1	−73.9	−68.8	−70.2
3	a	−161.9	−158.7	−151.8	−132.8
	b	108.4	110.9	111.8	121.4
	c	238.3	236.7	239.9	239.9
	w. a.	−100.4	−97.5	−91.7	−75.1
4	a	−66.9	−60.1	−54.2	−53.8
	b	51.5	55.0	55.4	57.3
	c	−185.3	−185.2	−184.5	−201.7
	w. a.	−54.4	−48.7	−44.2	−45.0
5	a	−230.6	−225.0	−226.9	−228.0
	b	−363.8	−357.1	−356.8	−340.0
	w. a.	−273.3	−267.3	−268.6	−263.9
6	a	−247.0	−241.0	−234.3	−226.1
	b	−200.9	−202.2	−195.4	−187.6
	c	−188.9	−189.7	−183.6	−179.3
	d	160.7	161.5	159.1	167.3
	w. a.	−160.0	−158.7	−153.5	−146.4

¹ Weighted average for a compound.

The inclusion of dispersion corrections into DFT calculations did not lead to a straightforward improvement of the calculated and experimental rotations. While they had a noticeable effect on the conformational analysis, the dispersion corrections did not affect the calculated ORs. For comparison, we recalculated optical rotations at the B3PW91/aug-cc-pVDZ level for dispersion-corrected geometries, and the results are given in Table 9.

Table 9. Calculated optical rotations in ethyl acetate for dispersion-corrected geometries.

Comp.	Conformer	aug-cc-pVDZ
1	a	24.3
2	a	101.7
	b	−222.9
	c	−341.7
	d	185.5
	w. a. ¹	−139.9
3	a	−26.0
	b	179.2
	w. a.	−10.6
4	a	−60.1
	b	55.0
	c	−185.2
	w. a.	−55.3
5	a	−257.2
	b	−191.6
	w. a.	−255.5
6	a	−335.4
	b	217.5
	w. a.	−292.9

¹ Weighted average for a compound.

While some minor improvement can be seen for compounds **1**, **4**, and **5**, for the other compounds, the agreement between the calculated and experimental optical rotations worsened, most significantly for compound **6**.

Comparing the basis sets used, it can be seen that the quadruple- ζ aug-cc-pVQZ basis set provides the best agreement between the calculated and experimental data. However, it is also the most time consuming. Table 10 lists the average CPU task times for the basis sets used.

Table 10. Average CPU task times for OR calculations.

Basis Set	Time [d]
6-311++G(2d,p)	0.5
aug-cc-pVDZ	0.5
aug-cc-pVTZ	10
aug-cc-pVQZ	>70

It is clear that the quadruple- ζ basis set is very expensive, even when used with multiple CPUs. For this reason, we concluded that the triple- ζ basis set has the best price/performance ratio for routine calculations of OR.

It must be emphasized that the signs of optical rotations were correctly predicted in all cases, and the calculations of OR can thus be used for the determination of absolute configurations, even for conformationally flexible compounds. Furthermore, it can be seen that optical rotations are extremely sensitive to minor changes in geometry and are suitable for the assessment of conformer populations during conformational analysis.

4. Conclusions

Based on successful applications of optical rotation calculations for the determination of the absolute configurations of various compounds, at least the rigid ones, we chose an opposite approach for the study of the conformational analysis of conformationally flexible molecules. As optical rotation is extremely sensitive to the 3D geometry of a compound, even small changes in the rotation of exocyclic groups can lead to dramatic changes in optical rotation. For this reason, we decided to use optical rotation as an evaluator of the conformational analysis results of conformationally flexible molecules. We performed a detailed computational conformational analysis of six flexible salicylamide-based compounds. In the initial step, we used the conformation search utility, which found hundreds of conformations for each compound. These were then optimized in two steps, and Boltzmann populations were calculated. This yielded 1–4 conformations for each molecule, and, finally, optical rotations were calculated as weighted averages of rotations for each populated conformer. For their DFT calculation, the B3PW91 functional was used with several basis sets including diffuse functions. If we assume that the optical rotations were calculated exactly, we employed an excellent tool for the assessment of conformational analysis. Of the six compounds for which experimental optical rotations were known, for two of them (**1** and **2**), the agreement between the calculated and experimental rotations were excellent. Compound **1** proved to be rigid and existed in one conformer only. For compound **2**, three populated conformers were found, two of them having negative optical rotations and one having positive rotations. It is clear that the conformers and their populations were calculated exactly in this case. For compounds **3** and **4**, the agreement between the experimental and calculated rotations was moderate. We can conclude that only minor discrepancies in populations occurred in this case. The worst agreement was found for compounds **5** and **6**. All the populated conformers of these compounds had highly negative rotations, while the experimental values were only slightly negative, i.e., -64.8° and -73.8° , respectively. It is evident that changes in populations could not improve the agreement between the experimental and calculated values substantially in this case and that it is probable that some conformers with only slight negative optical rotations or positive ORs were missed during the conformational analysis. The

inclusion of dispersion corrections into the DFT optimizations had a noticeable effect on the calculated geometries and their populations; however, a clear and straightforward improvement of the calculated optical rotations was not observed. Finally, we proved that the optical rotations calculated with the quadruple- ζ aug-cc-pVQZ basis set were the best but, unacceptably, too time consuming and that the triple- ζ basis set yielded optimum performance.

Author Contributions: Conceptualization I.R., A.I. and J.J.; methodology I.R.; software I.R.; investigation I.R., K.P., A.I. and J.J.; resources I.R., K.P., A.I. and J.J.; writing—original draft preparation I.R., K.P., A.I. and J.J.; funding acquisition I.R., A.I. and J.J. All authors have read and agreed to the published version of the manuscript.

Funding: This work was supported by the grant of the Ministry of Education, Youth and Sports of the Czech Republic for specific university research (A1_FPBT_2023_003). Computational resources were provided by the e-INFRA CZ project (ID:90254) supported by the Ministry of Education, Youth and Sports of the Czech Republic. This research was also supported by the Slovak Research and Development Agency (VEGA 1/0116/22) and by the Ministry of Education, Science, Research and Sports of the Slovak Republic and the Slovak Academy of Sciences (APVV-22-0133).

Institutional Review Board Statement: Not applicable

Informed Consent Statement: Not applicable.

Data Availability Statement: The data presented in this study are available on request from the corresponding author.

Conflicts of Interest: The authors declare no conflicts of interest.

References

1. Devinsky, F. Chirality and the origin of life. *Symmetry* **2021**, *13*, 2277. [CrossRef]
2. Ceramella, J.; Iacopetta, D.; Franchini, A.; De Luca, M.; Saturnino, C.; Andreu, I.; Sinicropi, M.S.; Catalano, A. A look at the importance of chirality in drug activity: Some significative examples. *Appl. Sci.* **2022**, *12*, 10909. [CrossRef]
3. Zhou, Y.; Wu, S.; Zhou, H.; Huang, H.; Zhao, J.; Deng, Y.; Wang, H.; Yang, Y.; Yang, J.; Luo, L. Chiral pharmaceuticals: Environment sources, potential human health impacts, remediation technologies and future perspective. *Environ. Int.* **2018**, *121*, 523–537. [CrossRef] [PubMed]
4. Silvestri, I.P.; Colbon, P.J.J. The growing importance of chirality in 3D chemical space exploration and modern drug discovery approaches for Hit-ID: Topical innovations. *ACS Med. Chem. Lett.* **2021**, *12*, 1220–1229. [CrossRef]
5. Abram, M.; Jakubiec, M.; Kaminski, K. Chirality as an important factor for the development of new antiepileptic drugs. *ChemMedChem* **2019**, *14*, 1744–1761. [CrossRef] [PubMed]
6. McGown, A.; Nafie, J.; Otayfah, M.; Hassell-Hart, S.; Tizzard, G.J.; Coles, S.J.; Banks, R.; Marsh, G.P.; Maple, H.J.; Kostakis, G.E.; et al. Chirality: A key parameter in chemical probes. *RSC Chem. Biol.* **2023**, *4*, 716–721. [CrossRef] [PubMed]
7. Jung, W.; Kwon, J.; Cho, W.; Yeom, J. Chiral biomaterials for nanomedicines: From molecules to supraparticles. *Pharmaceutics* **2022**, *14*, 1951. [CrossRef]
8. Cho, N.H.; Guerrero-Martinez, A.; Ma, J.; Bals, S.; Kotov, N.A.; Liz-Marzan, L.M.; Nam, K.T. Bioinspired chiral inorganic nanomaterials. *Nat. Rev. Bioeng.* **2023**, *1*, 88–106. [CrossRef]
9. Rosenfeld, L. Quantenmechanische Theorie der Natürlichen OptischenAktivität von Flüssigkeiten und Gasen. *Z. Phys.* **1928**, *52*, 161–174. [CrossRef]
10. Grauso, L.; Teta, R.; Esposito, G.; Menna, M.; Mangoni, A. Computational prediction of chiroptical properties in structure elucidation of natural products. *Nat. Prod. Rep.* **2019**, *36*, 1005–1030. [CrossRef]
11. Crawford, T.D.; Tam, M.C.; Abrams, M.L. The current state of ab initio calculations of optical rotation and electronic circular dichroism spectra. *J. Phys. Chem. A* **2007**, *111*, 12057–12068. [CrossRef] [PubMed]
12. Li, A.; Sun, X.; Liu, L. Action of salicylic acid on plant growth. *Front. Plant Sci.* **2022**, *13*, 878076. [CrossRef] [PubMed]
13. Salicylic Acid, DrugBank. Available online: <https://go.drugbank.com/drugs/DB00936> (accessed on 5 December 2023).
14. Dotto, C.; Lombarte Serrat, A.; Ledesma, M.; Vay, C.; Ehling-Schulz, M.; Sordelli, D.O.; Grunert, T.; Buzzola, F. Salicylic acid stabilizes *Staphylococcus aureus* biofilm by impairing the agr quorum-sensing system. *Sci. Rep.* **2021**, *11*, 2953. [CrossRef] [PubMed]
15. Almolhim, H.; Elhassanny, A.E.M.; Abutaleb, N.S.; Abdelsattar, A.S.; Seleem, M.N.; Carlier, P.R. Substituted salicylic acid analogs offer improved potency against multidrug-resistant *Neisseria gonorrhoeae* and good selectivity against commensal vaginal bacteria. *Sci Rep.* **2023**, *13*, 14468. [CrossRef]
16. Sykes, E.M.E.; White, D.; McLaughlin, S.; Kumar, A. Salicylic acids and pathogenic bacteria: New perspectives on an old compound. *Can. J. Microbiol.* **2024**, *70*, 1–14. [CrossRef]

17. Aspirin, DrugBank. Available online: <https://go.drugbank.com/drugs/DB00945> (accessed on 5 December 2023).
18. Mesalazine, DrugBank. Available online: <https://go.drugbank.com/drugs/DB00244> (accessed on 5 December 2023).
19. Niclosamide, DrugBank. Available online: <https://go.drugbank.com/drugs/DB06803> (accessed on 5 December 2023).
20. Rafoxanide, NIH—Inxight Drugs. Available online: <https://drugs.ncats.io/drug/22F4FLA7DH> (accessed on 5 December 2023).
21. Closantel, NIH—Inxight Drugs. Available online: <https://drugs.ncats.io/drug/EUL532EI54> (accessed on 5 December 2023).
22. Jiang, H.; Li, A.M.; Ye, J. The magic bullet: Niclosamide. *Front. Oncol.* **2022**, *12*, 1004978. [[CrossRef](#)]
23. Singh, S.; Weiss, A.; Goodman, J.; Fisk, M.; Kulkarni, S.; Lu, I.; Gray, J.; Smith, R.; Sommer, M.; Cheriyan, J. Niclosamide—A promising treatment for COVID-19. *Br. J. Pharmacol.* **2022**, *179*, 3250–3267. [[CrossRef](#)]
24. Kratky, M.; Vinsova, J. Salicylanilide ester prodrugs as potential antimicrobial agents—A review. *Curr. Pharm. Des.* **2011**, *17*, 3494–3505. [[CrossRef](#)]
25. Kratky, M.; Vinsova, J.; Novotna, E.; Mandikova, J.; Wsol, V.; Trejtnar, F.; Ulmann, V.; Stolarikova, J.; Fernandes, S.; Bhat, S.; et al. Salicylanilide derivatives block *Mycobacterium tuberculosis* through inhibition of isocitrate lyase and methionine aminopeptidase. *Tuberculosis* **2012**, *92*, 434–439. [[CrossRef](#)]
26. Wang, W.; Qin, Z.; Zhu, D.; Wei, Y.; Li, S.; Duan, L. Synthesis, bioactivity evaluation, and toxicity assessment of novel salicylanilide ester derivatives as cercaricides against *Schistosoma japonicum* and molluscicides against *Oncomelania hupensis*. *Antimicrob. Agents Chemother.* **2015**, *60*, 323–331. [[CrossRef](#)]
27. He, P.; Wang, W.; Sanogo, B.; Zeng, X.; Sun, X.; Lv, Z.; Yuan, D.; Duan, L.; Wu, Z. Molluscicidal activity and mechanism of toxicity of a novel salicylanilide ester derivative against *Biomphalaria* species. *Parasit. Vectors* **2017**, *10*, 383. [[CrossRef](#)] [[PubMed](#)]
28. Garcia, C.; Burgain, A.; Chaillot, J.; Pic, E.; Khemiri, I.; Sellam, A. A phenotypic small-molecule screen identifies halogenated salicylanilides as inhibitors of fungal morphogenesis, biofilm formation and host cell invasion. *Sci. Rep.* **2018**, *8*, 11559. [[CrossRef](#)] [[PubMed](#)]
29. Angom, R.S.; Zhu, J.; Wu, A.T.H.; Sumitra, M.R.; Pham, V.; Dutta, S.; Wang, E.; Madamsetty, V.S.; Perez-Cordero, G.D.; Huang, H.S.; et al. LCC-09, a novel salicylanilide derivative, exerts anti-inflammatory effect in vascular endothelial cells. *J. Inflamm. Res.* **2021**, *14*, 4551–4565. [[CrossRef](#)] [[PubMed](#)]
30. Imramovsky, A.; Ferriz, J.M.; Pauk, K.; Kratky, M.; Vinsova, J. Synthetic route for the preparation of 2-hydroxy-*N*-[1-(2-hydroxyphenylamino)-1-oxoalkan-2-yl]benzamides. *J. Comb. Chem.* **2010**, *12*, 414–416. [[CrossRef](#)] [[PubMed](#)]
31. Alazemi, A.M.; Dawood, K.M.; Al-Matar, H.M.; Tohamy, W.M. Microwave-assisted chemoselective synthesis and photophysical properties of 2-arylaazo-biphenyl-4-carboxamides from hydrazonals. *RSC Adv.* **2023**, *13*, 25054–25068. [[CrossRef](#)] [[PubMed](#)]
32. Lal, J.; Ramalingam, K.; Meena, R.; Ansari, S.B.; Saxena, D.; Chopra, S.; Goyal, N.; Reddy, D.N. Design and synthesis of novel halogen rich salicylanilides as potential antileishmanial agents. *Eur. J. Med. Chem.* **2023**, *246*, 114996. [[CrossRef](#)] [[PubMed](#)]
33. Kauerova, T.; Perez-Perez, M.J.; Kollar, P. Salicylanilides and their anticancer properties. *Int. J. Mol. Sci.* **2023**, *24*, 1728. [[CrossRef](#)]
34. Imramovsky, A.; Pesko, M.; Monreal-Ferriz, J.; Kralova, K.; Vinsova, J.; Jampilek, J. Photosynthesis-inhibiting efficiency of 4-chloro-2-(chlorophenylcarbamoyl)phenyl alkylcarbamates. *Bioorg. Med. Chem. Lett.* **2011**, *21*, 4564–4567. [[CrossRef](#)]
35. Imramovsky, A.; Stepankova, S.; Vanco, J.; Pauk, K.; Monreal-Ferriz, J.; Vinsova, J.; Jampilek, J. Acetylcholinesterase-inhibiting activity of salicylanilide *N*-alkylcarbamates and their molecular docking. *Molecules* **2012**, *17*, 10142–10158. [[CrossRef](#)]
36. Song, Q.; Li, Y.; Cao, Z.; Qiang, X.; Tan, Z.; Deng, Y. Novel salicylamide derivatives as potent multifunctional agents for the treatment of Alzheimer’s disease: Design, synthesis and biological evaluation. *Bioorg. Chem.* **2019**, *84*, 137–149. [[CrossRef](#)]
37. Kratky, M.; Jaklova, K.; Stepankova, S.; Svrckova, K.; Pflgr, V.; Vinsova, J. *N*-[3,5-Bis(trifluoromethyl)phenyl]-5-bromo-2-hydroxybenzamide analogues: Novel acetyl- and butyrylcholinesterase inhibitors. *Curr. Top. Med. Chem.* **2020**, *20*, 2094–2105. [[CrossRef](#)]
38. Macielag, M.J.; Demers, J.P.; Fraga-Spano, S.A.; Hlasta, D.J.; Johnson, S.G.; Kanojia, R.M.; Russell, R.K.; Sui, Z.; Weidner-Wells, M.A.; Werblood, H.; et al. Substituted salicylanilides as inhibitors of two-component regulatory systems in bacteria. *J. Med. Chem.* **1998**, *41*, 2939–2945. [[CrossRef](#)] [[PubMed](#)]
39. Otevrel, J.; Mandelova, Z.; Pesko, M.; Guo, J.; Kralova, K.; Sersen, F.; Vejsova, M.; Kalinowski, D.; Kovacevic, Z.; Coffey, A.; et al. Investigating the spectrum of biological activity of ring-substituted salicylanilides and carbamoylphenylcarbamates. *Molecules* **2010**, *15*, 8122–8142. [[CrossRef](#)] [[PubMed](#)]
40. Lee, I.Y.; Gruber, T.D.; Samuels, A.; Yun, M.; Nam, B.; Kang, M.; Crowley, K.; Winterroth, B.; Boshoff, H.I.; Barry, C.E. Structure-activity relationships of antitubercular salicylanilides consistent with disruption of the proton gradient via proton shuttling. *Bioorg. Med. Chem.* **2013**, *21*, 114–126. [[CrossRef](#)] [[PubMed](#)]
41. Vinsova, J.; Kozic, J.; Kratky, M.; Stolarikova, J.; Mandikova, J.; Trejtnar, F.; Buchta, V. Salicylanilide diethyl phosphates: Synthesis, antimicrobial activity and cytotoxicity. *Bioorg. Med. Chem.* **2014**, *22*, 728–737. [[CrossRef](#)] [[PubMed](#)]
42. Kushkevych, I.; Kollar, P.; Ferreira, A.L.; Palma, D.; Duarte, A.; Lopes, M.M.; Bartos, M.; Pauk, K.; Imramovsky, A.; Jampilek, J. Antimicrobial effect of salicylamide derivatives against intestinal sulfate-reducing bacteria. *J. Appl. Biomed.* **2016**, *14*, 125–130. [[CrossRef](#)]
43. Paraskevopoulos, G.; Monteiro, S.; Vosatka, R.; Kratky, M.; Navratilova, L.; Trejtnar, F.; Stolarikova, J.; Vinsova, J. Novel salicylanilides from 4,5-dihalogenated salicylic acids: Synthesis, antimicrobial activity and cytotoxicity. *Bioorg. Med. Chem.* **2017**, *25*, 1524–1532. [[CrossRef](#)]

44. Alhashimi, M.; Mayhoub, A.; Seleem, M.N. Repurposing salicylamide for combating multidrug-resistant *Neisseria gonorrhoeae*. *Antimicrob. Agents Chemother.* **2019**, *63*, e01225-19. [[CrossRef](#)]
45. Copp, J.N.; Pletzer, D.; Brown, A.S.; Van der Heijden, J.; Miton, C.M.; Edgar, R.J.; Rich, M.H.; Little, R.F.; Williams, E.M.; Hancock, R.E.W.; et al. Mechanistic understanding enables the rational design of salicylanilide combination therapies for Gram-negative infections. *mBio* **2020**, *11*, e02068-20. [[CrossRef](#)]
46. Pop, B.; Ionuț, I.; Marc, G.; Vodnar, D.C.; Pîrnau, A.; Vlase, L.; Oniga, O. Development of new 2-methyl-4-salicylamide thiazole derivatives: Synthesis, antimicrobial activity evaluation, lipophilicity and molecular docking study. *Farmacia* **2021**, *69*, 724–731. [[CrossRef](#)]
47. Imramovsky, A.; Pesko, M.; Kralova, K.; Vejsova, M.; Stolarikova, J.; Vinsova, J.; Jampilek, J. Investigating spectrum of biological activity of 4- and 5-chloro-2-hydroxy-N-[2-(arylamino)-1-alkyl-2-oxoethyl]benzamides. *Molecules* **2011**, *16*, 2414–2430. [[CrossRef](#)] [[PubMed](#)]
48. Kratky, M.; Vinsova, J. Salicylanilide N-monosubstituted carbamates: Synthesis and in vitro antimicrobial activity. *Bioorg. Med. Chem.* **2016**, *24*, 1322–1330. [[CrossRef](#)]
49. Baranyai, Z.; Kratky, M.; Vinsova, J.; Szabo, N.; Senoner, Z.; Horvati, K.; Stolarikova, J.; David, S.; Bosze, S. Combating highly resistant emerging pathogen *Mycobacterium abscessus* and *Mycobacterium tuberculosis* with novel salicylanilide esters and carbamates. *Eur. J. Med. Chem.* **2015**, *101*, 692–704. [[CrossRef](#)] [[PubMed](#)]
50. Ienascu, I.M.C.; Obistoiu, D.; Popescu, I.M.; Stefanut, M.N.; Gyongyi, O.; Jurca, C.; Ciavoi, G.; Bechir, E.S.; Bechir, F.; Cata, A. In vitro testing of salicylanilide derivatives against some fungal and bacterial strains. *Rev. Chim.* **2019**, *70*, 1496–1499. [[CrossRef](#)]
51. Ienascu, I.M.C.; Cata, A.; Stefanut, M.N.; Popescu, I.; Rusu, G.; Sfirloaga, P.; Ursu, D.; Mosoarca, C.; Dabici, A.; Danciu, C.; et al. Novel chloro-substituted salicylanilide derivatives and their β -cyclodextrin complexes: Synthesis, characterization, and antibacterial activity. *Biomedicines* **2022**, *10*, 1740. [[CrossRef](#)] [[PubMed](#)]
52. Pindjakova, D.; Pilarova, E.; Pauk, K.; Michnova, H.; Hosek, J.; Magar, P.; Cizek, A.; Imramovsky, A.; Jampilek, J. Study of biological activities and ADMET-related properties of salicylanilide-based peptidomimetics. *Int. J. Mol. Sci.* **2022**, *23*, 11648. [[CrossRef](#)]
53. Panda, S.S.; Kumari, S.; Dixit, M.; Sharma, N.K. N-Salicyl-AA-n-picolamide foldameric peptides exhibit quorum sensing inhibition of *Pseudomonas aeruginosa* (PA14). *ACS Omega* **2023**, *8*, 30349–30358. [[CrossRef](#)]
54. Jorda, R.; Magar, P.; Hendrychova, D.; Pauk, K.; Dibus, M.; Pilarova, E.; Imramovsky, A.; Krystof, V. Novel modified leucine and phenylalanine dipeptides modulate viability and attachment of cancer cells. *Eur. J. Med. Chem.* **2020**, *188*, 112036. [[CrossRef](#)]
55. Xu, J.; Kim, H.; Dong, J.; Chen, H.; Xu, J.; Ma, R.; Zhou, M.; Wang, T.; Shen, Q.; Zhou, J. Structure-activity relationship studies on O-alkylamino-tethered salicylamide derivatives with various amino acid linkers as potent anticancer agents. *Eur. J. Med. Chem.* **2022**, *234*, 114229. [[CrossRef](#)]
56. Soukaina, E.; Al-Zaqri, N.; Warad, I.; Ichou, H.; Yassine, K.; Guenoun, F.; Bouachrine, M. Novel antiproliferative inhibitors from salicylamide derivatives with dipeptide moieties using 3D-QSAR, molecular docking, molecular dynamic simulation and ADMET studies. *J. Mol. Struct.* **2023**, *1282*, 135219. [[CrossRef](#)]
57. Advanced Chemistry Development, Inc. *ACD/Name, ver. 12.01*; Advanced Chemistry Development, Inc.: Toronto, ON, Canada, 2009.
58. Hypercube Inc. *HyperChem, Release 8.0.3 for Windows, Molecular Modeling System*; Hypercube Inc.: Waterloo, ON, Canada, 2007.
59. Becke, A.D. Density-functional thermochemistry. III. The role of exact exchange. *J. Chem. Phys.* **1993**, *98*, 5648–5652.
60. Perdew, J.P.; Chevary, J.A.; Vosko, S.H.; Jackson, K.A.; Pederson, M.R.; Singh, D.J.; Fiolhais, C. Atoms, molecules, solids, and surfaces: Applications of the generalized gradient approximation for exchange and correlation. *Phys. Rev. B Condens. Matter Mater. Phys.* **1992**, *46*, 6671–6687. [[CrossRef](#)] [[PubMed](#)]
61. Barone, V.; Cossi, M. Quantum calculation of molecular energies and energy gradients in solution by a conductor solvent model. *J. Phys. Chem. A* **1998**, *102*, 1995–2001. [[CrossRef](#)]
62. Cossi, M.; Rega, N.; Scalmani, G.; Barone, V. Energies, structures, and electronic properties of molecules in solution with the C-PCM solvation model. *J. Comput. Chem.* **2003**, *24*, 669–681. [[CrossRef](#)] [[PubMed](#)]
63. Grimme, S.; Antony, J.; Ehrlich, S.; Krieg, H. A consistent and accurate ab initio parameterization of density functional dispersion correction (DFT-D) for the 94 elements H-Pu. *J. Chem. Phys.* **2010**, *132*, 154104. [[CrossRef](#)]
64. Frisch, M.J.; Trucks, G.W.; Schlegel, H.B.; Scuseria, G.E.; Robb, M.A.; Cheeseman, J.R.; Scalmani, G.; Barone, V.; Petersson, G.A.; Nakatsuji, H.; et al. *Gaussian 16, Revision B.01*; Gaussian, Inc.: Wallingford, CT, USA, 2016.
65. Stephens, P.J.; Devlin, F.J.; Cheeseman, J.R.; Frisch, M.J.; Mennucci, B.; Tomasi, J. Prediction of optical rotation using density functional theory: 6,8-dioxabicyclo [3.2.1]octanes. *Tetrahedron Asymmetry* **2000**, *11*, 2443–2448. [[CrossRef](#)]
66. Cheeseman, J.R.; Frisch, M.J.; Devlin, F.J.; Stephens, P.J. Hartree-Fock and density functional theory ab initio calculation of optical rotation using GIAOs: Basis set dependence. *J. Phys. Chem. A* **2000**, *104*, 1039–1046. [[CrossRef](#)]
67. Stephens, P.J.; Devlin, F.J.; Cheeseman, J.R.; Frisch, M.J. Calculation of optical rotation using density functional theory. *J. Phys. Chem. A* **2001**, *105*, 5356–5371. [[CrossRef](#)]

-
68. Stephens, P.J.; McCann, D.M.; Cheeseman, J.R.; Frisch, M.J. Determination of absolute configurations of chiral molecules using ab initio time-dependent density functional theory calculations of optical rotation: How reliable are absolute configurations obtained for molecules with small rotations? *Chirality* **2005**, *17*, S52–S64. [[CrossRef](#)]
 69. Mennucci, B.; Tomasi, J.; Cammi, R.; Cheeseman, J.R.; Frisch, M.J.; Devlin, F.J.; Gabriel, S.; Stephens, P.J. Polarizable continuum model (PCM) calculations of solvent effects on optical rotations of chiral molecules. *J. Phys. Chem. A* **2002**, *106*, 6102–6113. [[CrossRef](#)]

Disclaimer/Publisher’s Note: The statements, opinions and data contained in all publications are solely those of the individual author(s) and contributor(s) and not of MDPI and/or the editor(s). MDPI and/or the editor(s) disclaim responsibility for any injury to people or property resulting from any ideas, methods, instructions or products referred to in the content.